Submission intended as an Article in the Methods section of MBE

Non-phylogenetic identification of co-evolving genes for reconstructing the archaeal Tree of Life

L. Thibério Rangel[1], Shannon M. Soucy[2], João Carlos Setubal[3], Johann Peter Gogarten[4], Gregory P. Fournier[1]

[1] Department of Earth, Atmospheric & Planetary Sciences, Massachusetts Institute of Technology, Cambridge, MA, USA

[2] Department of Biomedical Data Science, Geisel School of Medicine, Dartmouth College, Hanover, NH, USA

[3] Departamento de Bioquímica, Instituto de Química, Universidade de São Paulo, São Paulo, Brasil

[4] Department of Molecular and Cell Biology, University of Connecticut, Storrs, CT, USA

Corresponding author: Gregory P. Fournier, g4nier@mit.edu

Abstract

Assessing the phylogenetic compatibility between individual gene families is a crucial and often computationally demanding step in many phylogenomics analyses. Here we describe the Evolutionary Similarity Index (I_{ES}) to assess shared evolution between gene families using a weighted Orthogonal Distance Regression applied to sequence distances. This approach allows for straightforward pairing of paralogs between co-evolving gene families without resorting to multiple tests, or *a priori* assumptions of molecular interactions between protein products from assessed genes. The utilization of pairwise distance matrices, while less informative than phylogenies, circumvents error-prone comparisons between trees whose topologies are inherently uncertain. Analyses of simulated tree datasets showed that I_{ES} was more accurate and less susceptible to phylogenetic noise than existing tree-based methods (Robinson-Foulds and geodesic distance) for assessing evolutionary signal compatibility. Applying I_{ES} to a real dataset of 1,322 genes from 42 archaeal genomes identified eight major clusters of co-evolving gene families. Four of these clusters included genes with a taxonomic distribution across all archaeal phyla, while other clusters included a subset of taxa that do not map to generally accepted archaeal clades, indicating possible shared horizontal transfers by co-evolving gene families. We identify one strongly connected set of 62 co-evolving genes occurring as both single-copy and multiple homologs per genome, with compatible evolutionary histories closely matching previously published species trees for Archaea. An I_{ES} implementation is available at https://github.com/lthiberiol/evolSimIndex.

Introduction

Phylogenies reconstructed from single genes are known to poorly reflect the underlying history of whole genomes, as the detectable phylogenetic signal from an isolated locus cannot be extrapolated to represent whole genomes (Dagan and Martin 2006; Bapteste et al. 2009; Koonin et al. 2009). To this effect, it has become common practice to estimate species' evolutionary histories by concatenating multiple sequence alignments of core genes, which greatly increases the number of sites available for phylogenetic inference. The preference towards concatenating core genes is due its expected to horizontal gene transfer (HGT) (Thomas and Nielsen 2005; Sorek et al. 2007; Popa and Dagan 2011); however, despite the lower frequency of HGT among some gene families, horizontal exchange still takes place within their history. The slow

substitution rate and corresponding high sequence conservation of the core genome can become a liability due to the increase in neutral and nearly-neutral HGT at the genus and species level (Papke and Gogarten 2012; Shapiro et al. 2012). Biases in horizontal exchange between closely related genomes may even reinforce the misconception of strong HGT resistance (Andam et al. 2010; Andam and Gogarten 2011).

Given these processes, surveying evolutionary compatibility between different gene families is important to minimize conflicting evolutionary signals combined during phylogenomic reconstruction. Multiple strategies have been proposed to assess similarities between the phylogenetic signals found within individual genes- e.g., Robinson-Foulds bipartition compatibility (RF) (Robinson and Foulds 1981) and geodesic distance (Kimmel and Sethian 1998; Kupczok et al. 2008; Owen and Provan 2011). The majority of these methods are based on straightforward comparisons between tree topologies (Kunin et al. 2005; Leigh et al. 2008; Puigbò et al. 2009; Mirarab et al. 2014; Gori et al. 2016). While an intuitive solution, comparisons between tree topologies require phylogenetic trees of all assessed gene families to be accurately reconstructed, adding a substantial computational cost to a reliable execution of an already computationally demanding task. Furthermore, the vastness of tree space, combined with the inherent uncertainty of phylogenetic reconstruction, constitutes an error-rich layer in tree-based evolutionary similarity assessments.

Accounting for uncertainty-based variations in tree topology (i.e., bipartition support) further increases the computational burden and decreases the resolution of the evaluated phylogenetic signal (e.g., collapsing low support bipartitions or weighing them based on support). A proposed solution to bypass the computational cost of tree similarity assessments is Pearson's correlation coefficient (r) between evolutionary distance matrices (Goh et al. 2000; Pazos and Valencia 2001; Novichkov et al. 2004; Rangel et al. 2019). Despite its application in protein-protein interaction studies, the sensitivity of Pearson's r to phylogenetic noise and the granularity of its estimates have yet to be compared to those of tree-based metrics. Unlike tree-based comparisons, methods based on Pearson's r enable simple implementations to detect co-evolving gene families with histories complicated by multiple homologs within genomes by estimating correlation coefficients using all possible pairings of paralogs between gene families (Gertz et al. 2003; Ramani and Marcotte 2003). Direct Coupling Analysis (DCA) has also been used to pair gene copies between co-evolving gene families (Gueudré et al. 2016), but despite

positive results the assumption that products of co-evolving genes must be structurally associated exerts extreme burden toward its general applicability.

New approaches

Here we propose the Evolutionary Similarity Index (I_{ES}) as a metric of evolutionary history similarities based on weighted Orthogonal Distance Regression (wODR) between evolutionary pairwise distance matrices. Simulations show that wODR performed very similarly to Pearson correlation coefficients, with the added advantage of more robust estimated relationships between gene families. This approach does not require multiple tests where there are gene duplications. We show that evolutionary similarity estimates from wODR display a linear relationship with stepwise perturbations in tree topologies. More common estimates of tree similarity, such as RF and geodesic distances, tend to overestimate the impact of topology changes, and consequently are significantly more susceptible to phylogenetic noise. We further assessed evolutionary similarities across 1,322 archaeal gene families and detected significant evolutionary incompatibilities between conserved single-copy genes, as well as a clear central evolutionary tendency involving 62 gene families that occur as both single and multiple-copies across genomes.

Methodology

Orthogonal Distance Regression (ODR) is an errors-in-variables regression method that accounts for measurement errors in both explanatory and response variables (Boggs et al. 1987), instead of attributing all errors in the expected values exclusively to the response variable, as performed by Ordinary Least Squares (OLS). While OLS regressions seek to minimize the sum of squared residuals of the response variable, ODR minimizes the sum of squared residuals from each data point obtained by the combination of explanatory and response variables. Novichkov et al. (Novichkov et al. 2004) assessed the compatibility between the evolutionary history of genes with a reference genomic evolutionary history using Pearson's *r* and estimates of an OLS regression's intercept. This latter extra step when compared to other implementations using Pearson's *r* (Ramani and Marcotte 2003; Izarzugaza et al. 2008; Gueudré et al. 2016) is required

for a robust inference given that at a hypothetical time exactly after genome divergence, distances between homologs in both genomes must be zero. The approach proposed by Novichkov et al. requires two key assumptions that restrict the general applicability of evolutionary assessments of empirical datasets: 1) there must exist a reference history to which gene histories are compared; and 2) there are no errors in reference distances between genomes.

The approach described here is based on ODR. Its modelling of errors within both assessed variables decreases the necessity of a well-established reference distance to compare gene family pairwise distances against. Consequently, errors-in-variables approaches (e.g., ODR) are better suited to compare pairwise evolutionary distances between two gene families, where *a priori*, there is no clear separation between explanatory and response variables. Independently weighing residuals from each data point provides a framework less susceptible to underestimating overall evolutionary similarities due to few homologs with high incompatibility. Our implementation also fits wODR while forcing the intercept through the origin, which avoids overfitting the linear regression model to the detriment of coherent evolutionary assumptions.

Algorithm explanation

Tree-based evolutionary distance assessment algorithms are not generally capable of pairing genes between two gene families when at least one family contains multiple gene copies (Stamatakis 2006; Nguyen et al. 2015; Gori et al. 2016; Huerta-Cepas et al. 2016). Pearson *r* implementations either rely on multiple tests (Gertz et al. 2003; Ramani and Marcotte 2003; Izarzugaza et al. 2008) or on predicting structural interaction between gene products (Gueudré et al. 2016). Our implementation performs an initial wODR using all pairs of genes within the same genome, one from each assessed gene family, and reports gene pairs that minimize the sum of squared residuals. As exemplified in Fig. 1, a hypothetical *gene1* occurs exclusively as single copy across 10 genomes (Fig. 1, tree1), while *gene2* has an extra copy within genome *J* (Fig. 1, tree2). In order to identify which copy of *gene2* in *J* (*j1* or *j2*) better represents their shared evolution we compare *gene1* pairwise distances involving *j* with *gene2* pairwise distances involving *j1* and j*2*. Consequently, to do that we must duplicate *J*'s rows and columns in matrix1 to match matrix2 dimensions (Fig. 1, matrix1). The scatter plot in Fig. 1 highlights pairwise distances involving *j1* in blue and *j2* in red, and as shown by the fitted wODR regression, *gene2* pairwise distances involving *j1* fits better to the expected linear association between matrix1 and

matrix2 than pairwise distances involving *j2*. The smallest sum of residuals obtained by the *j1* homolog of *gene2* correctly pairs it with *J*'s *gene1* homolog, while *j2*'s *gene2* homolog is likely a product of HGT from a shared common ancestor of *A* and *B* . When both gene families occur in multiples within the same genome, all pairs of unique loci are reported. Once best matching genes from each gene family are paired, or if both occur exclusively as single copy, a final wODR is performed using paired homologs from each gene family. wODR is performed through the SciPy (Virtanen et al. 2020) API of ODRPACK (Boggs et al. 1989). Initial weights of pairwise distance are estimated as the inverse of residuals obtained from geometric distance regression with no intercept and slope equal to s_Y/s_X, where s_Y and s_X are standard deviations from the regressed distance matrices.

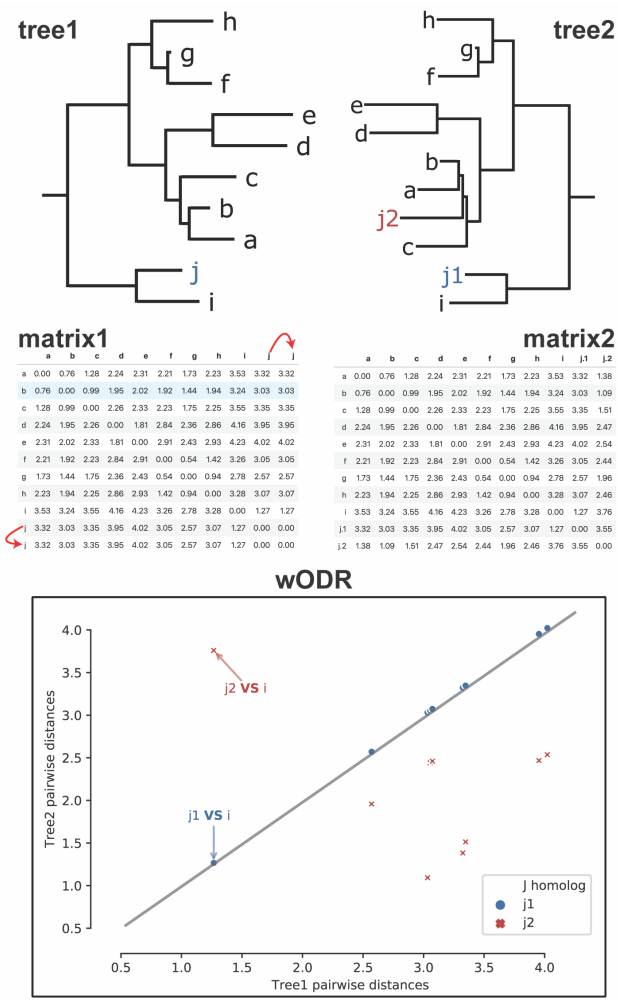

Fig. 1 Steps for I_{ES} estimation between gene families containing multiple gene copies. *tree1* and *tree2* are phylogenetic trees of two hypothetical gene families, *gene1* and *gene2*, respectively. *matrix1* and *matrix2* contain pairwise evolutionary distances between taxa from their respective gene families. The red arrows in *matrix1* highlight the duplication of pairwise distances involving the *j* homolog of *gene1* necessary to match dimensions of the two matrices. The wODR scatterplot fits the linear

relationships between distances from both gene families, and highlights distances related to the *j1* homolog of *gene2* in blue and related to the *j2* homolog in red. Arrows also highlight pairwise distances homologs in genomes *J* and *I* from both gene families.

Given that regression models only account for data points equally represented in both assessed variables, gene losses and duplications are not directly accounted for when comparing evolutionary histories through wODR. To incorporate unequal genomic occurrence between gene families to our proposed measurement of evolutionary similarity, the wODR Coefficient of Determination, i.e. R^2, is adjusted by the Bray-Curtis Index(I_{BC}). I_{BC} is defined as $1 - D_{BC}$, where is the D_{BC} is Bray-Curtis Dissimilarity (Bray and Curtis 1957) calculated from absolute genome counts in each gene family. From hereon we will refer to the wODR $R^2 \times I_{BC}$ product as I_{ES}. Continuing with the example depicted in Fig. 1, despite *gene1* and *gene2* identical genomic occurrence, their copy numbers diverge within genome *J*, which as mentioned before, arose from a horizontal exchange of *gene2*. To reflect this difference in evolutionary events within gene family histories in the proposed I_{ES}, the resulting wODR $R^2 = 1$ is adjusted using an $I_{BC} = 0.95$.

Statistics and data analysis

Pandas Python library (McKinney 2010) was used to manipulate pairwise distance matrices and for generating condensed versions of the matrices submitted to wODR model. Effect size (*f*) hypothesis tests of differences between distributions were obtained using Common Language statistics (McGraw and Wong 1992), and p-value correction for multiple tests was performed using False Discovery Rate implementation in StatsModels Python library (Seabold and Perktold 2010).

Data Simulation

We constructed ten simulated datasets, each one containing 50 trees generated from stepwise random Subtree Prune and Regraft (SPR) transformations. Each dataset contains one initial random rooted tree with 50 taxa generated by ETE3 (Huerta-Cepas et al. 2016). To obtain the remaining 49 trees, the initial tree (*tree_1*) undergoes a series of 49 consecutive SPR transformations in such a way that *tree_1* differs from *tree_2*, *tree_3*, and *tree_n* by 1, 2, and *n* SPR transformations, respectively. At each SPR the branch leading to the regrafted clade undergoes two transformations to simulate changes in substitution rate after an HGT event. The

first transformation multiplies the branch length by a random uniform variable ranging from 0 to 1, simulating at which point during the branch's history the transfer occurred. The second transformation multiplies by a random gamma distributed variable ($\alpha = \beta = 100$), simulating changes in substitution rates in the recipient clade after said transfer. All simulated trees are available in Supplementary Material.

All simulated trees were also used to generate sequence simulations using INDELible (Fletcher and Yang 2009) (Supplementary Material). Phylogenetic trees and pairwise distance matrices were reconstructed using IQTree (Nguyen et al. 2015) using the LG+G model.

Archaeal empirical dataset

Complete genome sequences of 42 Archaea were downloaded from NCBI GenBank (Supplementary Table S1), and clustering of homologous proteins performed using the orthoMCL (Li et al. 2003) implementation available at GET_HOMOLOGUES (Contreras-Moreira and Vinuesa 2013; Vinuesa and Contreras-Moreira 2015). Archaea were selected as the test dataset since the evolutionary relationships between some major groups are well-established, while others remain contested. Furthermore, many sets of archaeal metabolic genes have a strong phyletic dependence (e.g., methanogenesis among Euryarchaeota) more easily permitting tests of gene co-evolution at different phylogenetic distances. Evolutionary similarity comparisons were restricted to homologous groups present in at least 10 genomes. Pairwise maximum likelihood distances between homologous proteins were generated using IQTree and LG+G model.

Enrichment of gene functions among co-evolving gene families were performed using StringDB API (Szklarczyk et al. 2019). For each genome, homologs from co-evolving gene families were submitted independently for enrichment assessment. Retrieved protein annotations are available in the Supplementary Material.

Geodesic and Robinson-Foulds distance calculations

Geodesic distances between single copy gene families (both simulated and real datasets) were calculated using the treeCl Python package (Gori et al. 2016). RF distances between single copy gene families were calculated by ETE3.

Results and Discussion

Simulated dataset

Evolutionary histories between simulated gene families were compared to each other using three distinct metrics: RF, geodesic distance, and I_{ES}. Results reported by all three approaches successfully identified the monotonic increase in SPR operations from a starting tree (Fig. 2 and Supplementary Fig. S1). Measurements obtained from RF and geodesic approaches, however, frequently overestimated the impact of SPR transformations between two gene families, leading to a fast saturation of dissimilarities between evolutionary histories (Fig. 2B and Fig. 2C). The dissimilarity saturations detected by RF and geodesic measurements occur as they fail to identify the decreasing similarity between two trees separated by more than 15 to 20 SPR transformations, or even 10 SPR in some replicates (simulation replicate #1, Supplementary Fig. S1). Both of these approaches rely on the proportion of compatible bipartitions shared by two trees, which is very susceptible to small changes at deep bipartitions, where changing one single leaf can potentially create fully incompatible bipartition tables.

In contrast, I_{ES} displayed a robust linear relationship with the number of SPR transformations between gene families ($\bar{r} = -0.87$, Fig. 2A). The lower level of information assessed by I_{ES}, pairwise distance matrices instead of dichotomic trees, is less susceptible to dissimilarity saturation, corresponding to a more linear relation between expected and observed changes in evolutionary histories. Furthermore, I_{ES} is much more efficient, computationally. Tree reconstruction of the alignment simulated from *tree_1* of the first simulation replicate (50 taxa and 500 sites with no indels) under LG+G model in a single thread by IQTree took 80.604 seconds, while exclusively calculating pairwise distance matrix for the same alignment took 1.713 seconds. Both computations were performed in a 3 GHz Intel Xeon W. The difference in computing time of almost 50x, without bipartition support assessment, shows another, practical advantage for assessing evolutionary similarity through I_{ES} in large datasets.

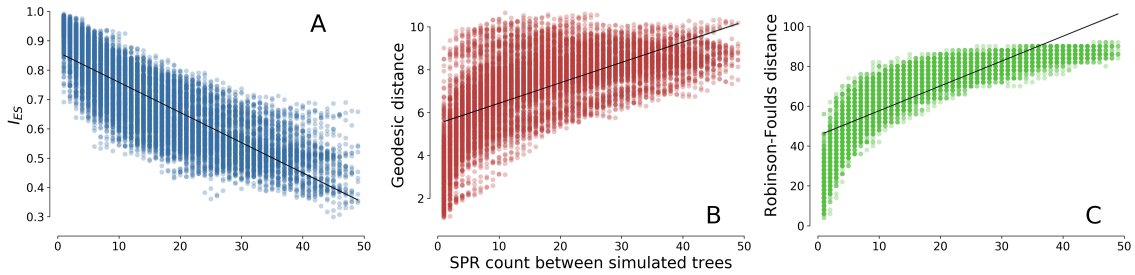

Fig. 2 Scatter plot of evolutionary similarity metrics against number of SPR transformations between simulated gene families from all ten replicates. Solid black lines are estimated from OLS regressions between number of SPR transformations and evolutionary similarity metrics. All three scatter plots display the number of SPR transformations between two trees in the X-axis, while varying the evolution similarity metric displayed in the Y-axis. A) displays wODR R^2 between distance matrices of simulated gene families in the Y-axis, B) displays geodesic distances between trees reconstructed from each simulated alignment, and C) displays RF distances estimated from the same trees.

Robustness assessment between approaches

The dichotomic pattern in a cladogram is extremely susceptible to phylogenetic uncertainty, combined with the vast tree space available for 50 taxa, causing topological variations from phylogenetic uncertainty to not be directly differentiated from real deviations in evolutionary history (Szöllosi et al. 2013). The simpler information used to estimate I_{ES} (i.e., pairwise Maximum Likelihood distances) is less prone to such uncertainty as it bypasses forming hypotheses about the evolutionary relationships between taxa. This assumption is corroborated by pairwise comparisons within bootstrap replicates, where I_{ES} correctly detected replicates as such, i.e., virtually identical to each other, while RF and geodesic measures failed to identify the common nature of bootstrap replicates. In addition to its accurate predictions, I_{ES} consistently displayed very little variance within its estimates between bootstrap replicates.

Each sequence simulation alignment was used to generate 10 bootstrap replicates. Pairwise comparisons between 10 bootstrap replicates summed up to 45 comparisons within a single alignment, given that we simulated a total of 500 alignments, we assessed 22,500 pairwise comparisons between bootstrap replicates across all simulated datasets. I_{ES} values correctly identified bootstrap replicates as sharing virtually identical evolutionary histories, $\overline{R^2} = 0.96$, and did so very consistently (CV = 1.39%, where CV stands for Coefficient of Variation). Despite successfully identifying increasing evolutionary changes between simulated trees, RF distances inconsistently predicted similarities between histories of bootstrapped trees (CV =

57.45%), as variations in bootstrapped alignments caused small perturbations in reconstructed tree topologies, and subsequent underestimation of evolutionary similarity between bootstrap replicates (an average of 18% incompatible bipartitions). While more prone to saturation than RF and more with variance than I_{ES} estimates, geodesic distance displayed an acceptable degree of variation within its estimates ($\mathrm{CV} = 14.97\%$). Geodesic distances yielded an average of 1.25 between bootstrap replicates, which cannot be directly translated to a proportion of incompatible bipartitions between trees.

Evolutionary similarities within archaeal gene families

In order to test I_{ES} performance when estimating shared evolution in an empirical set of gene families, we evaluated 1,322 families of homologous proteins assembled from annotated CDSs extracted from 42 archaeal genomes (Supplementary Table S1). This empirical dataset contains conserved and accessory gene families with different sizes due to gene losses, duplications, and transfers.

I_{ES} was estimated for all pairwise combinations of gene families present in at least 10 genomes, with 2,142 out of 748,712 comparisons having I_{ES} values of at least 0.7. Pairs of gene families with an $I_{ES} \geq 0.7$ were added as nodes to a weighted network with its estimated I_{ES} value as an edge connecting both gene families. In total 419 unique archaeal gene families were added to the network, while the remaining 908 gene families did not display any $I_{ES} \geq 0.7$ with other gene families. The resulting evolutionary similarity network (Fig. 3) is heavily imbalanced, with just 11% of nodes involved in 50% of network edges and the majority of gene families, 68%, did not display I_{ES} above the 0.7 threshold with other gene families, suggesting a general incompatibility of phylogenetic signal, or lack thereof to detect its compatibility with others. However, the high edge concentration within just a few nodes suggests a strong central evolutionary backbone (Puigbò et al. 2009) preserved among a few gene families, from which the evolutionary trajectories of others have diverged. Similarities between evolutionary histories, as estimated by I_{ES}, are strongly associated with genomic linkage ($p = 6.18e^{-75}$ and $f = 0.86$). Gene families frequently occurring in each other's genomic vicinity (i.e., fewer than 10,000 bp apart in at least 21 genomes) displayed significantly greater I_{ES} relative to pairs of gene families that were further apart (i.e., more than 100,000 bp apart in at least 21 genomes) (Fig. 4a).

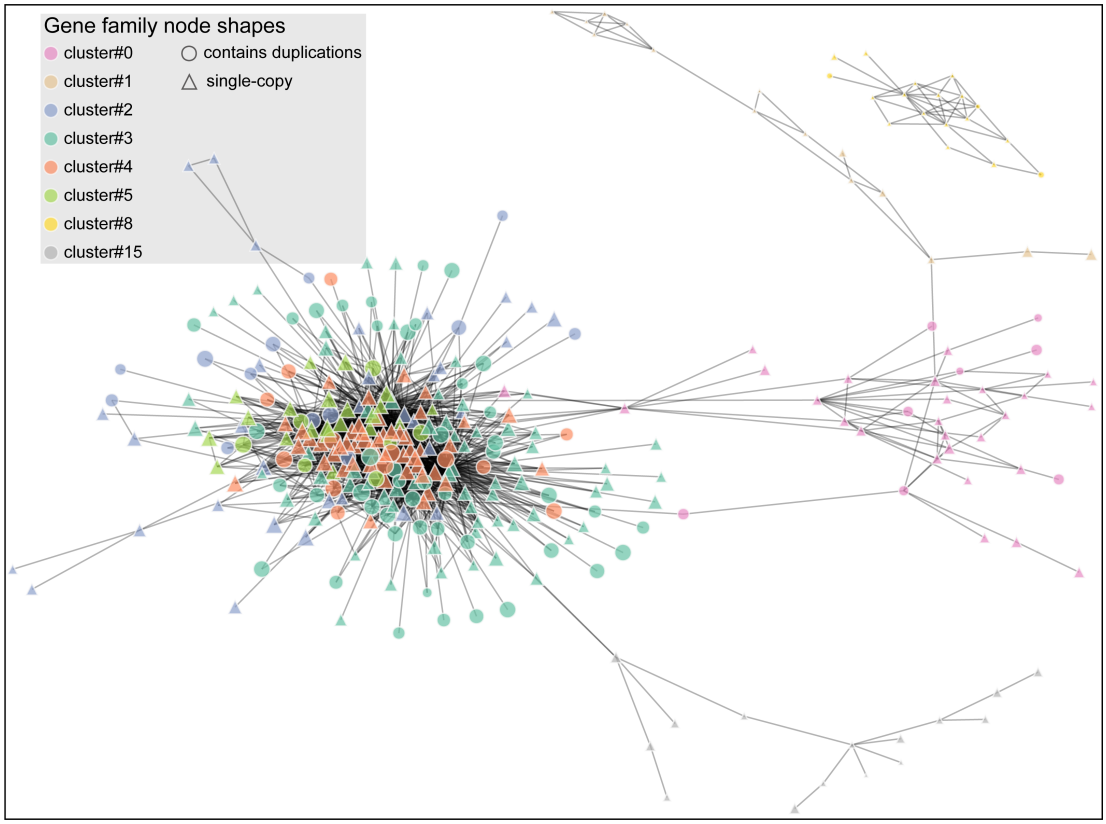

Fig. 3 Gene family co-evolution network, each node represents a gene family, and edges connecting nodes represent shared evolutionary history ($I_{ES} \geq 0.7$). Nodes in the same colors are identified as co-evolving by Louvain community detection. Triangular nodes represent single-copy genes, and circular ones are gene families containing gene duplications. Clusters of co-evolving gene families with less than ten members are not represented.

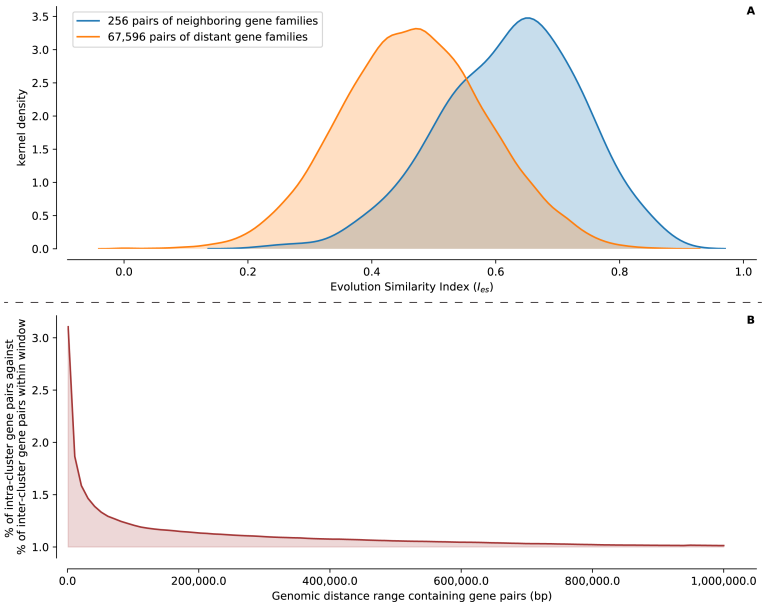

Fig. 4 A) distributions of I_{ES} between pairs of genes within 10,000 bp of each other in blue and between pairs of genes apart by at least 100,000 bp in orange. Neighboring gene pairs displayed significantly more similar evolutionary histories than non-

neighboring gene pairs. B) ratio between the proportion of co-evolving gene pairs and non-co-evolving gene pairs, Y-axis, occurring within genomic windows, X-axis. 100 window sizes were assessed ranging from 1,000 bp to 1,000,000 bp.

Clusters of co-evolving gene families

Shared patterns of evolution across gene families were assessed using Louvain community detection (Blondel et al. 2008), which reported eight major clusters with at least 10 similarly evolving gene families (Fig. 6). Each of these clusters comprise gene families sharing common evolutionary trends and paths, although the co-evolution assumption based on I_{ES} estimates and the clustering process is agnostic of specific shared evolutionary events or their causes. That said, the association between genomic linkage and co-evolution is very pronounced. Across small nucleotide distances between loci, linkage is a strong predictor of gene co-evolution, but its predictive power rapidly decreases as the number of nucleotides between two given loci increase (Fig. 4b), displaying a linear log-log relationship (Supplementary Fig. S2). Comparisons between intra- and inter-cluster genomic linkage showed that the proportion of co-evolving genes within 1,000 bp of each other is three times the proportion of non-co-evolving genes within the same window. Increasing the surveilled genomic window decreases the difference between proportions; within a 10,000 bp window, the proportion of co-evolving genes is reduced to 1.8 the proportion of non-co-evolving, and at a 100,000 bp window this difference in proportions falls to 1.2 (Fig. 4b).

Among the eight clusters with ten or more co-evolving gene families four are comprised of mostly core genes, and four are composed of mostly accessory genes (Fig. 6). The four clusters of co-evolving core genes (cluster#2, cluster#3, cluster#4, and cluster#5) are promising candidates for reconstructing the phylogenetic signal of vertical inheritance within Archaea. Core genes composing these co-evolving clusters are broadly distributed among archaeal clades and generally occur as single copies within genomes, although can also be found in multiples. Clusters of co-evolving accessory genes (cluster#0, cluster#1, cluster#8, and cluster#15 in Fig. 6) do not reflect specific archaeal clades, instead they link polyphyletic clades with biased distribution caused by HGTs and/or gene losses shared by co-evolving gene families. For example, cluster#0 is well represented amongst Euryarchaeota and hyperthermophilic TACK; cluster#15 comprises gene families with shared evolutionary histories mainly occurring within Crenarachaeota and hyperthermophilic Euryarchaeota; co-evolving accessory gene families in

cluster#1 and cluster#8 display congruent signals tying methanogenic Euryarchaeota with Thaumarchaeota and Asgardarchaeota, respectively.

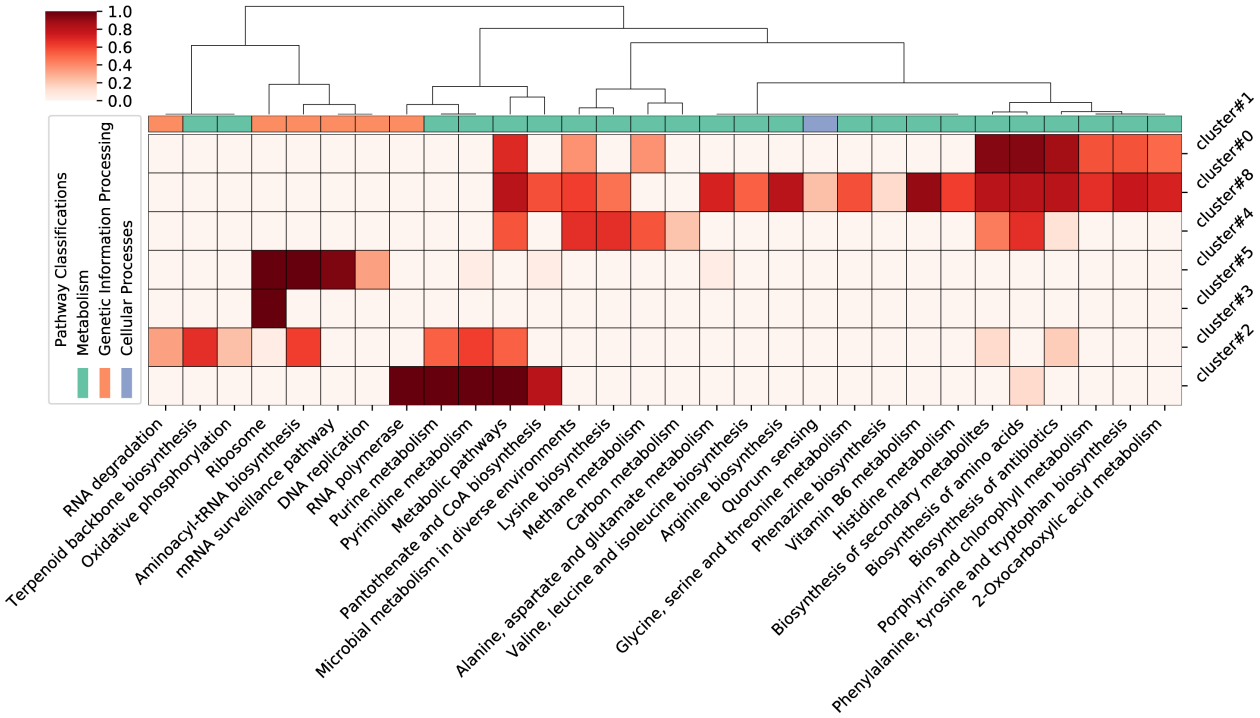

Fig. 5 Heatmap of enriched KEGG Pathways, columns, within clusters of co-evolving gene families, rows. Shades of red represent the proportion of genomes with detected KEGG Pathway enrichment within its homologs of co-evolving gene families. Columns and rows were clustered using complete linkage and correlation coefficients. KEGG Pathways enriched in less than 10% of genomes in which co-evolving genes occur are not reported. Cluster#15 did not report significant enrichment of KEGG Pathways.

CDSs from 21 out of 42 sampled genomes have functional annotation available in StringDB (Supplementary Material), and through its API we identified annotated KEGG Pathways enriched within homologs of co-evolving gene families from each genome. In the dendrogram and heatmap depicted in Fig. 5 we clearly identify two sets of opposing clusters of co-evolving gene families: accessories (top three rows) and core (bottom four rows), and their associations with genetic information processing and metabolism KEGG Pathways (indicated by column color in the top row). All four clusters of co-evolving core gene families are enriched with KEGG Pathways related to genetic information processing (e.g., Ribosome, DNA replication, and Aminoacyl-tRNA biosynthesis). Co-evolving accessory gene families on the other hand tend to be enriched with KEGG Pathways related to metabolism (e.g., Methane metabolism, Microbial metabolism in diverse environments, and Biosynthesis of antibiotics in

Fig. 5). It is also important to emphasize the opposite pattern of enrichment and depletion of KEGG Pathways between clusters of core and accessory genes. KEGG Pathways related to metabolism display minor enrichment signal within core co-evolving gene families, and KEGG Pathways related to genetic information processing are not enriched within clusters of co-evolving accessory genes (Fig. 5). Co-evolving accessory genes comprised within cluster#1, whose occurrence is restricted to methanogenic Euryarchaeota and Thaumarchaeota, are enriched for methane metabolism within six genomes. Similarly, gene families from in cluster#8, restricted to methanogenic Euryarchaeota and Asgardarchaeota, are also enriched in methane metabolism in five genomes (Fig. 5). The biased occurrence of co-evolving gene families within cluster#1 and cluster#8 towards methanogenic Archaea (Fig. 6) and the enrichment of methane metabolism within gene families from both clusters (Fig. 5) support a possible origin of these genes within Euryarchaeota with subsequent independent horizontal transfer to other archaeal clades.

The horizontal exchange of genes commonly accepted as resistant to HGT is exemplified by the split of extended core-genes in four distinct co-evolving clusters (Fig. 3 and Fig. 7). In regard to the distribution in extended core-genes among co-evolving clusters, cluster#4 contains the greatest number of extended core-genes, 44 out of 102. Closeness centrality measures ($\tilde{C} = 0.56$) and node strength divided by cluster size ($\tilde{S} = 0.19$) also suggest that cluster#4 gene families have a stronger and cohesive co-evolution signal than gene families from other clusters (Supplemental Fig S3). In addition, the phylogeny obtained from concatenated cluster#4 gene families (Fig. 6) is the most similar to the extended core phylogeny among phylogenies from all co-evolving clusters (Fig. 7).

The 44 extended core genes contained within co-evolving cluster#4 are better representatives of the extended core-genome phylogenetic signal than extended core-genes not within this cluster ($p = 3.78e^{-6}$ and $f = 0.74$, Supplementary Fig. S4). The great similarity between cluster#4 and extended core phylogenies (Fig. 6 and Fig. 7) indicate that gene families comprising cluster#4 are the major contributors to the vertical evolution signal estimated from the extended core tree. Though cluster#4 comprises only 60.7% of the number gene families used to reconstruct the extended core tree, it is still able to provide well supported bipartitions (Fig. 6), corroborating the shared compatible signal within its co-evolving gene families. Such

overall compatibility between phylogenetic signals is not likely present within other extended core genes (Fig. 7), which are scattered across four distinct co-evolving clusters.

Common and distinct evolutionary trends between co-evolving clusters

Among clusters of co-evolving core gene families, cluster#4 and cluster#5 are the most evenly represented across archaeal groups, while cluster#2 and cluster#3 are poorly distributed among DPANN (Fig. 6). All four co-evolving clusters have low frequency within Thaumarchaeota archaeon SCGC AB-539-E09, and only gene families from cluster#2 and cluster#4 are significantly present in Thermoplasmatales archaeon SCGC AB-539-N05. All four clusters display very similar overall phylogenies, varying mainly within the organization of Euryarchaeota (Fig. 6 and Supplementary Material). All four co-evolving clusters reconstructed the monophyly of Euryarchaeota, with the exception of cluster#2, which placed *Pyrococcus furiosus*, *Thermococcus kodakarensis*, *Methanocaldococcus jannaschii*, *Methanothermobacter thermautotrophicus*, and *Methanopyruus kandleri* together as sister to Asgardarchaeota+TACK. Only cluster#4 recovered the monophyly of Methanomicrobia as sister to Halobacteria, with the other three co-evolving clusters placing Halobacteria within Methanomicrobia.

All four core co-evolving clusters robustly identified Asgardarchaeota as sister to TACK (Fig. 6), with small variation in the Asgardarchaeota phylogeny, and cluster#5 placing Korarchaeota at the base of the TACK super-phylum. When assessing all-versus-all evolutionary similarities between clusters of co-evolving core genes, the phylogenetic history reconstructed from cluster#4 is the least dissimilar to the other three (Fig. 7). This shortest path from cluster#4's evolutionary trajectory to all others corroborates the hypothesis that cluster#4 best represents the backbone of the vertical inheritance signal, a central point from which others have diverged (Fig. 7). In general, the overall high I_{ES} estimates between co-evolving clusters suggest that despite composing distinct clusters, gene histories between clusters are generally congruent, with deviations reflecting small divergences potentially representing genes with specific sets of reticulate histories.

Phylogenetic trees obtained from co-evolving accessory gene families in cluster#0, cluster#1, cluster#8, and cluster#15 reconstructed all represented archaeal phyla as monophyletic (except for *P. furiosus* in Euryarchaeota in cluster#0, Supplementary Fig. S5), suggesting a shared common origin of accessory co-evolving genes from each cluster by all genomes from the

same phylum. Although the monophyly of archaeal phyla within trees of co-evolving accessory genes does not permit an accurate prediction of the directionality of possible inter-phyla HGTs, intra-phylum distances congruent to the vertical inheritance signal can be used to evaluate the fitness of inter-phylum distances under a wODR model (Supplemental Fig. S6, S8, S10, and S11). When compared to pairwise distances expected from vertical inheritance, inter-phylum distances that significantly differ from estimates obtained by intra-phylum distances may be attributed to HGT acquisition by one of the phyla in question. For each cluster of co-evolving accessory genes, we assessed wODR of its pairwise distances against the vertical evolution estimated from cluster#4.

When comparing pairwise distances obtained from cluster#1 against cluster#4, distances between Euryarchaeota and Thaumarchaeota are consistently placed bellow the estimated regression line (Supplementary Fig. S6 and S7). This suggests that cluster#1 genes were horizontally transferred between ancestors of both phyla, causing shorter evolutionary distances between phyla than expected if their homologs diverged from the vertical inheritance.

Inter-phyla distances between Euryarchaeota and Crenarchaeota obtained from cluster#0 fit the evolutionary rate expected using intra-phylum distances for this co-evolving cluster (Supplementary Fig. S8), suggesting that homologs from both phyla were vertically inherited from a common ancestor. On the other hand, cluster#0 inter-phyla distances involving Thaumarchaeota (Crenarchaeota to Thaumarchaeota and Euryarchaeota to Thaumarchaeota) are shorter than expected from the wODR using intra-phylum distances (Supplementary Fig. S8) and display significantly greater residuals than distances between Crenarchaeota and Euryarchaeota (Supplementary Fig. S9). The absence of cluster#0 genes among Asgardarchaeota and Korarchaeota and the short inter-phyla distances to Thaumarchaeota homologs suggest an extensive loss among missing clades and horizontal acquisition by the thaumarchaeal ancestor from either crenarchaeal or euryarchaeal donors.

Despite the occurrence of accessory genes from cluster#1 and cluster#8 in methanogenic Euryarchaeota (Fig. 6) and the enrichment of methane metabolism pathways (Fig. 5), evolutionary histories of both co-evolving clusters are not related (Fig. 3). Co-evolving genes in cluster#8 did not display $I_{ES} \geq 0.7$ outside its own cluster, constituting a separate connected component in the co-evolution network depicted in Fig. 3. That said, cluster#8 gene families display shorter Euryarchaeota-Asgardarchaeota distances when compared to cluster#4 distances,

but unlike cluster#0 and cluster#1, intra-Asgardarchaeota and intra-Euryarchaeota pairwise distances are not mutually compatible under a single linear regression (Supplemental Fig. S10). The lack of a strong wODR anchor in the form of intra-phyla distances suggests a more complex horizontal exchange history of cluster#8 genes, possibly involving intra-phylum HGTs, which we cannot accurately assess with the dataset used in this study. Cluster#15 co-evolving accessory genes are well distributed among Crenarchaeota, and its intra-phylum pairwise distances correspond to cluster#4 distances, but their patchy occurrence among Euryarchaeota and Korarchaeota (Fig. 6) does not permit a confident assessment of this cluster's evolutionary history (Supplementary Fig. S5).

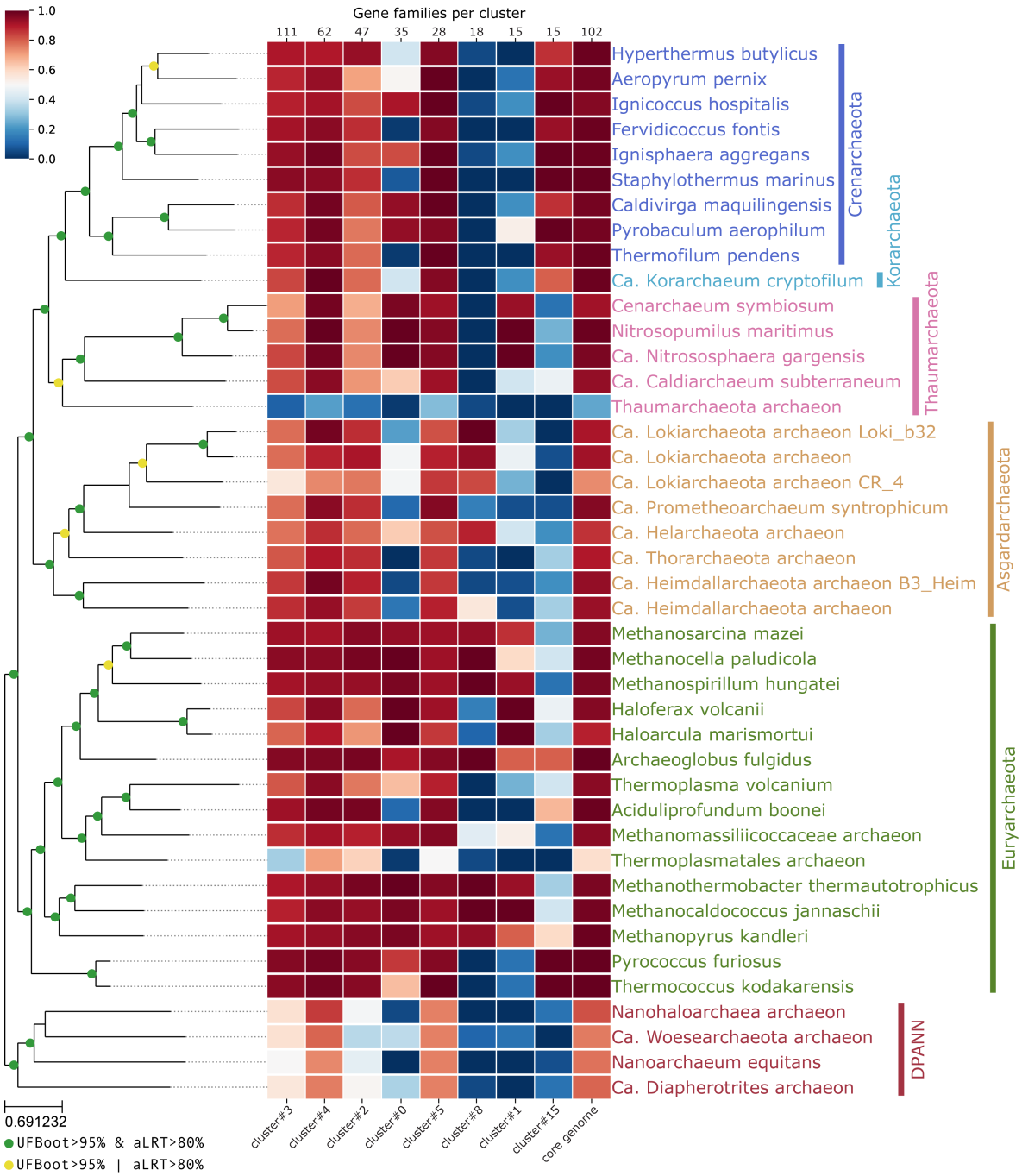

Fig. 6 Phylogenetic tree of Archaea reconstructed from 62 co-evolving genes within cluster#4. The phylogeny was obtained using LG+F+G+C60 evolutionary model from IQTree and each gene had its parameters independently estimated according to parameter "-sp". Bipartition supports were estimated using UFBoot and aLRT, each with 1,000 replicates, and bipartitions well supported by both methods are colored in green (UFBoot ≥ 95% and aLRT ≥ 80%), while bipartitions well supported by a single method are colored in yellow. Despite the addition of outgroups to Archaea (e.g. Bacteria) the tree is rooted in DPANN for the sake of visualization. The associated heatmap reflects the representation of co-evolving gene families amongst archaeal genomes.

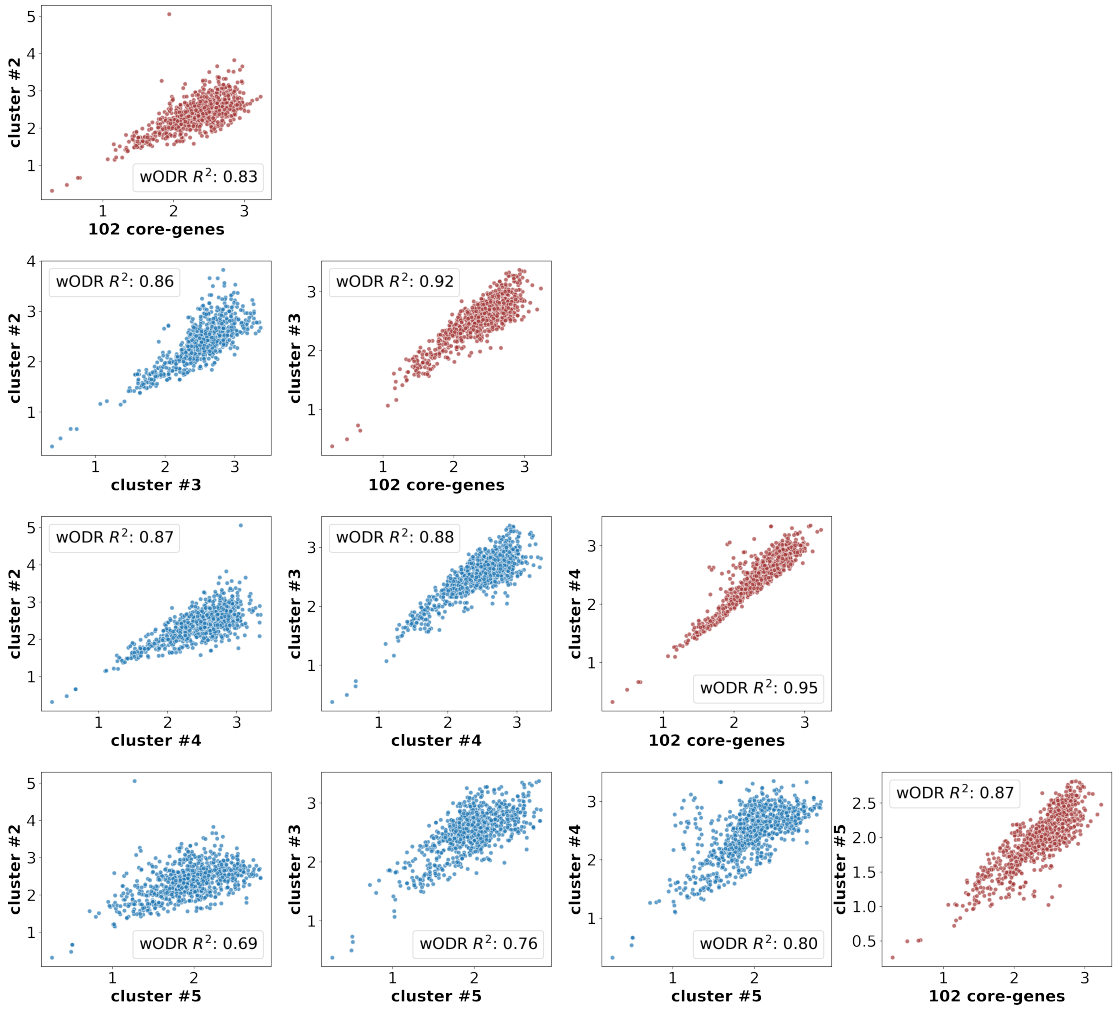

Fig. 7 Scatter plots of pairwise evolutionary distances reconstructed from each widely distributed gene family versus each other in blue. And in red, scatter plots of pairwise evolutionary distances reconstructed from each widely distributed gene family versus pairwise evolutionary distances reconstructed from 102 extended core gene families. Similarities between evolutionary histories of pairs of co-evolving clusters, and between co-evolving clusters and extended core genes were estimated by I_{ES}.

Conclusions

The results presented demonstrate the overall accuracy and robustness of I_{ES} estimates using both simulated and empirical datasets, as well as comparatively to common tools available to the community. Among the presented evidence, the clear identification of the strong association between genomic linkage and gene co-evolution based on I_{ES} estimates in itself constitutes an independent evidence of I_{ES} competence to assess shared evolutionary histories. In regard to its impact to phylogenomic analysis, reconstructing the vertical inheritance signal from

cluster#4 gene families provides a widely applicable improved alternative to analyses limited by conserved single copy genes.

One major consequence of co-evolution between gene families is their co-occurrence among genomes, given that if genes followed similar evolutionary trajectories, they are likely to be observed in comparable numbers within the same genomes. Despite similar performances of Pearson's *r* and wODR R^2, the detection of similar occurrence patterns among genomes in I_{ES} constitutes an important step towards more efficient co-evolution inference between genes. The utilization of wODR also imparts more robust statistical support not directly available to previous Pearson's *r* implementations. The ability to assess residuals of each datapoint independently also allows for evaluations of specific homologs, a useful tool for HGT detection. Future applications of I_{ES} can guide generation of sequence datasets for more accurate and robust species-tree inference, as well as the detection of significant clusters of gene families evolving in shared, yet reticulate, patterns.

Results presented here support I_{ES} as a superior proxy for evolutionary similarity between gene families, outperforming classical tree-based metrics. Comparisons between bootstrapped replicates within simulated datasets, which should be virtually identical, further corroborates the robustness of I_{ES} to phylogenetic uncertainty when compared to RF and geodesic distances.

Acknowledgements

This work was supported by Simons Foundation Collaboration on the Origins of Life Award #339603 and NSF Integrated Earth Systems Program Award #1615426 to GPF. SMS was supported through Geisel School of Medicine at Dartmouth's Center for Quantitative Biology through a grant from the National Institute of General Medical Sciences of the National Institutes of Health under Award Number P20GM130454.

References

Andam CP, Gogarten JP. 2011. Biased gene transfer and its implications for the concept of lineage. Biol. Direct [Internet] 6:47. Available from: http://www.pubmedcentral.nih.gov/articlerender.fcgi?artid=3191353&tool=pmcentrez&rendertype=abstract

Andam CP, Williams D, Gogarten JP. 2010. Biased gene transfer mimics patterns created through shared ancestry. Proc. Natl. Acad. Sci. U. S. A. [Internet] 107:10679–10684. Available from: http://www.pubmedcentral.nih.gov/articlerender.fcgi?artid=2890805&tool=pmcentrez&rendertype=abstract

Bapteste E, O'Malley M a, Beiko RG, Ereshefsky M, Gogarten JP, Franklin-Hall L, Lapointe F-J, Dupré J, Dagan T, Boucher Y, et al. 2009. Prokaryotic evolution and the tree of life are two different things. Biol. Direct [Internet] 4:34. Available from: http://www.pubmedcentral.nih.gov/articlerender.fcgi?artid=2761302&tool=pmcentrez&rendertype=abstract

Blondel VD, Guillaume J-L, Lambiotte R, Lefebvre E. 2008. Fast unfolding of communities in large networks. J. Stat. Mech. Theory Exp. [Internet] 2008:P10008. Available from: http://stacks.iop.org/1742-5468/2008/i=10/a=P10008?key=crossref.46968f6ec61eb8f907a760be1c5ace52

Boggs PT, Byrd RH, Schnabel RB. 1987. A Stable and Efficient Algorithm for Nonlinear Orthogonal Distance Regression. SIAM J. Sci. Stat. Comput. [Internet] 8:1052–1078. Available from: http://epubs.siam.org/doi/10.1137/0908085

Boggs PT, Donaldson JR, Byrd R h., Schnabel RB. 1989. Algorithm 676: ODRPACK: software for weighted orthogonal distance regression. ACM Trans. Math. Softw. [Internet] 15:348–364. Available from: http://dl.acm.org/doi/10.1145/76909.76913

Bray JR, Curtis JT. 1957. An Ordination of the Upland Forest Communities of Southern Wisconsin. Ecol. Monogr. [Internet] 27:325–349. Available from: http://doi.wiley.com/10.2307/1942268

Contreras-Moreira B, Vinuesa P. 2013. GET_HOMOLOGUES, a versatile software package for scalable and robust microbial pangenome analysis. Appl. Environ. Microbiol. [Internet] 79:7696–7701. Available from: http://www.pubmedcentral.nih.gov/articlerender.fcgi?artid=3837814&tool=pmcentrez&rendertype=abstract

Dagan T, Martin W. 2006. The tree of one percent. Genome Biol. 7.

Fletcher W, Yang Z. 2009. INDELible: A flexible simulator of biological sequence evolution. Mol. Biol. Evol. 26:1879–1888.

Gertz J, Elfond G, Shustrova A, Weisinger M, Pellegrini M, Cokus S, Rothschild B. 2003. Inferring protein interactions from phylogenetic distance matrices. Bioinformatics 19:2039–2045.

Goh CS, Bogan AA, Joachimiak M, Walther D, Cohen FE. 2000. Co-evolution of proteins with their interaction partners. J. Mol. Biol. 299:283–293.

Gori K, Suchan T, Alvarez N, Goldman N, Dessimoz C. 2016. Clustering Genes of Common Evolutionary History. Mol. Biol. Evol. [Internet] 33:1590–1605. Available from: http://mbe.oxfordjournals.org/content/early/2016/02/17/molbev.msw038.short?rss=1

Gueudré T, Baldassi C, Zamparo M, Weigt M, Pagnani A. 2016. Simultaneous identification of specifically interacting paralogs and interprotein contacts by direct coupling analysis. Proc. Natl. Acad. Sci. U. S. A. [Internet] 113:12186–12191. Available from: http://www.ncbi.nlm.nih.gov/pubmed/27729520

Huerta-Cepas J, Serra F, Bork P. 2016. ETE 3: Reconstruction, Analysis, and Visualization of Phylogenomic Data. Mol. Biol. Evol. [Internet] 33:1635–1638. Available from: https://academic.oup.com/mbe/article-lookup/doi/10.1093/molbev/msw046

Izarzugaza JMG, Juan D, Pons C, Pazos F, Valencia A. 2008. Enhancing the prediction of protein pairings between interacting families using orthology information. BMC Bioinformatics [Internet] 9:35. Available from: http://bmcbioinformatics.biomedcentral.com/articles/10.1186/1471-2105-9-35

Kimmel R, Sethian J a. 1998. Computing geodesic paths on manifolds. Proc. Natl. Acad. Sci. U. S. A. [Internet] 95:8431–8435. Available from: http://www.ncbi.nlm.nih.gov/pubmed/9671694

Koonin E V, Wolf YI, Puigbò P. 2009. The phylogenetic forest and the quest for the elusive tree of life. Cold Spring Harb. Symp. Quant. Biol. [Internet] 74:205–213. Available from: http://www.ncbi.nlm.nih.gov/pubmed/19687142

Kunin V, Goldovsky L, Darzentas N, Ouzounis CA. 2005. The net of life: reconstructing the microbial phylogenetic network. Genome Res. [Internet] 15:954–959. Available from: http://www.ncbi.nlm.nih.gov/pubmed/15965028

Kupczok A, von Haeseler A, Klaere S. 2008. An exact algorithm for the geodesic distance between phylogenetic trees. J. Comput. Biol. [Internet] 15:577–591. Available from: http://www.ncbi.nlm.nih.gov/pubmed/18631022

Leigh JW, Susko E, Baumgartner M, Roger AJ. 2008. Testing Congruence in Phylogenomic Analysis. Syst. Biol. [Internet] 57:104–115. Available from: http://sysbio.oxfordjournals.org/cgi/doi/10.1080/10635150801910436

Li L, Stoeckert CJ, Roos DS. 2003. OrthoMCL: identification of ortholog groups for eukaryotic genomes. Genome Res. [Internet] 13:2178–2189. Available from: http://www.ncbi.nlm.nih.gov/pubmed/12952885

McGraw KO, Wong SP. 1992. A common language effect size statistic. Psychol. Bull. [Internet] 111:361–365. Available from: http://doi.apa.org/getdoi.cfm?doi=10.1037/0033-2909.111.2.361

McKinney W. 2010. Data Structures for Statistical Computing in Python. In: p. 56–61. Available from: https://conference.scipy.org/proceedings/scipy2010/mckinney.html

Mirarab S, Bayzid MS, Bossau B, Warnow T. 2014. Statistical binning improves species tree estimation in the presence of gene tree heterogeneity. Science (80-.). [Internet] 346. Available from: http://dx.doi.org/10.1126/science.1250463

Nguyen L-T, Schmidt HA, von Haeseler A, Minh BQ. 2015. IQ-TREE: a fast and effective stochastic algorithm for estimating maximum-likelihood phylogenies. Mol. Biol. Evol. [Internet] 32:268–274. Available from: http://www.ncbi.nlm.nih.gov/pubmed/25371430

Novichkov PS, Omelchenko M V, Gelfand MS, Mironov A a, Wolf YI, Koonin E V. 2004. Genome-wide molecular clock and horizontal gene ransfer in bacterial evolution. J. Bacteriol. [Internet] 186:6575–6585. Available from: http://www.pubmedcentral.nih.gov/articlerender.fcgi?artid=516599&tool=pmcentrez&rendertype=abstract

Owen M, Provan JS. 2011. A Fast Algorithm for Computing Geodesic Distances in Tree Space. IEEE/ACM Trans. Comput. Biol. Bioinforma. [Internet] 8:2–13. Available from: http://ieeexplore.ieee.org/document/5396323/

Papke RT, Gogarten JP. 2012. Ecology. How bacterial lineages emerge. Science [Internet] 336:45–46. Available from: http://www.ncbi.nlm.nih.gov/pubmed/22491845

Pazos F, Valencia A. 2001. Similarity of phylogenetic trees as indicator of protein-protein interaction. Protein Eng. 14:609–614.

Popa O, Dagan T. 2011. Trends and barriers to lateral gene transfer in prokaryotes. Curr. Opin. Microbiol. [Internet] 14:615–623. Available from:

http://www.ncbi.nlm.nih.gov/pubmed/21856213
Puigbò P, Wolf YI, Koonin E V. 2009. Search for a “Tree of Life” in the thicket of the phylogenetic forest. J. Biol. [Internet] 8:59. Available from: http://www.ncbi.nlm.nih.gov/pubmed/19594957
Ramani AK, Marcotte EM. 2003. Exploiting the co-evolution of interacting proteins to discover interaction specificity. J. Mol. Biol. 327:273–284.
Rangel LT, Marden J, Colston S, Setubal JC, Graf J, Gogarten JP. 2019. Identification and characterization of putative Aeromonas spp. T3SS effectors.Antunes LCM, editor. PLoS One [Internet] 14:e0214035. Available from: https://dx.plos.org/10.1371/journal.pone.0214035
Robinson DF, Foulds LR. 1981. Comparison of phylogenetic trees. Math. Biosci. [Internet] 53:131–147. Available from: http://linkinghub.elsevier.com/retrieve/pii/0025556481900432
Seabold S, Perktold J. 2010. statsmodels: Econometric and statistical modeling with python. In: 9th Python in Science Conference.
Shapiro BJ, Friedman J, Cordero OX, Preheim SP, Timberlake SC, Szabó G, Polz MF, Alm EJ. 2012. Population genomics of early events in the ecological differentiation of bacteria. Science [Internet] 336:48–51. Available from: http://www.pubmedcentral.nih.gov/articlerender.fcgi?artid=3337212&tool=pmcentrez&rendertype=abstract
Sorek R, Zhu Y, Creevey C, Francino M. 2007. Genome-wide experimental determination of barriers to horizontal gene transfer. Science (80-.). [Internet] 318:1449–1452. Available from: http://www.sciencemag.org/content/318/5855/1449.short
Stamatakis A. 2006. RAxML-VI-HPC: maximum likelihood-based phylogenetic analyses with thousands of taxa and mixed models. Bioinformatics [Internet] 22:2688–2690. Available from: http://www.ncbi.nlm.nih.gov/pubmed/16928733
Szklarczyk D, Gable AL, Lyon D, Junge A, Wyder S, Huerta-Cepas J, Simonovic M, Doncheva NT, Morris JH, Bork P, et al. 2019. STRING v11: protein–protein association networks with increased coverage, supporting functional discovery in genome-wide experimental datasets. Nucleic Acids Res. [Internet] 47:D607–D613. Available from: https://academic.oup.com/nar/article/47/D1/D607/5198476
Szöllosi GJ, Rosikiewicz W, Boussau B, Tannier E, Daubin V. 2013. Efficient exploration of the

space of reconciled gene trees. Syst. Biol. 62:901–912.

Thomas CM, Nielsen KM. 2005. Mechanisms of, and barriers to, horizontal gene transfer between bacteria. Nat. Rev. Microbiol. [Internet] 3:711–721. Available from: http://dx.doi.org/10.1038/nrmicro1234

Vinuesa P, Contreras-Moreira B. 2015. Robust Identification of Orthologues and Paralogues for Microbial Pan-Genomics Using GET_HOMOLOGUES: A Case Study of pIncA/C Plasmids. In: p. 203–232. Available from: http://link.springer.com/10.1007/978-1-4939-1720-4_14

Virtanen P, Gommers R, Oliphant TE, Haberland M, Reddy T, Cournapeau D, Burovski E, Peterson P, Weckesser W, Bright J, et al. 2020. SciPy 1.0: fundamental algorithms for scientific computing in Python. Nat. Methods [Internet] 17:261–272. Available from: http://www.nature.com/articles/s41592-019-0686-2